A MULTI-SCALE MODEL FOR THE COMPUTER-AIDED DESIGN OF POLYMER COMPOSITES

Namin Jeong*, David W. Rosen
[1] School of Mechanical Engineering, Georgia Institute of Technology, Atlanta, GA, USA
* Corresponding author (specialnamin@gatech.edu)

Keywords: *multi-scale modeling, polymer composites, wavelet, surfacelet, computer-aided design*

1. Introduction

In engineering design, geometry and material can be separately specified at the traditional macroscale. However, at the micro- and meso-scales, material compositions become important in functional realization, such as in composites and functionally graded materials. A novel CAD system is under development that supports multiscale geometry and materials modeling which enables concurrent product-material design. We proposed a new multiscale geometric and materials modeling method that uses an implicit representation based on wavelets and their extension to efficiently capture internal and boundary information. This new approach enables integration of structure-property relationships for materials design. We call our modeling approach dual representation or dual-Rep [1]. In this paper, the surfacelet transform is defined, which consists of the Radon and wavelet transforms, in order to develop structure-property relationships. We demonstrate the methods with an example polymer nanocomposite material and illustrate structure-property model integration.

2. Geometric Modeling

Our objective is to develop a geometric model that can represent both part macroscale geometry and material microstructure; i.e., a multiscale geometry for computer-aided design of composite materials. Wavelets are the most common representation for multi-resolution modeling in the domain of 2D shape representation. Similar to Fourier analysis, wavelet analysis represents and approximates signals (or functions). The functional space for wavelet analysis is decomposed based on a scaling function $j(t)$ and a wavelet function $y(t)$ with one-dimensional variable t for multi-resolution analysis [2]:

$$y_{a,b}(t) = a^{-1/2} y\left(a^{-1}(t-b)\right) \qquad (1)$$

where a is a scaling (dilation) factor and b is a translation factor. In the geometric modeling domain, the wavelet transforms were used to describe planar curves with multiple resolutions.

Part and material microstructure boundaries can be viewed as surface singularities that are discontinuous in one direction while continuous in the other two directions in 3D space. Therefore, we propose new surfacelet basis functions for multiscale modeling [3]. Particularly, a 3D ridgelet (type of surfacelet) that represents plane singularities is defined as [4]

$$y_{a,b,\alpha,\beta}(r) = a^{-1/2} y\left(a^{-1}\begin{pmatrix} x\cos\beta\cos\alpha + \\ y\cos\beta\sin\alpha + z\sin\beta - b \end{pmatrix}\right) \qquad (2)$$

where $\mathbf{r} = (\mathbf{x}, \mathbf{y}, \mathbf{z})$ is the location in the domain Ω in the Euclidean space, $y: \mathbf{R} \to \mathbf{R}$ is a wavelet function, $r_{b,p}: \mathbf{R}^3 \to \mathbf{R}$ is a surface function so that $r_{b,p}(x, y, z) = 0$ implicitly defines a surface, with factor b and the shape parameter vector $\boldsymbol{p} \in \mathbf{R}^m$ determining the location and shape of surface singularities, respectively, and $\alpha \in [0, 2p)$ and $b \in [-p/2, p/2]$ are angular parameters corresponding to rotations.

We propose the dual-Rep model that uses both wavelet and surfacelet basis functions in order to model external part shapes as well as internal microstructural geometry boundaries. The approach to generating dual-Rep models of microstructure is to recognize microstructure features from stacks of 2D micro-scale images. The Radon transform is an effective method for representing line singularities in images [3]. The Radon transform was developed to reconstruct images from CT scans [5], which consist of sets of parallel scans where the source and sensor rotate around the target. We use this transform to fit surfacelet models to microstructures.

Then, by applying a wavelet transform to the results of the Radon transform, an image representation is produced that is potentially sparse and enables many image processing techniques to be applied.

Mathematically, the Radon transform in a domain Ω is the integral along the plane (represented as the dash line in 2D), which is perpendicular to a line at angle α, as illustrated in Fig. 5. The plane and the line intersect at a point which has the radial distance μ from the origin. Varying μ results in a vector of integral values, $I_\alpha(\mu)$ in 2D and $I_{\alpha,\beta}(\mu)$ in 3D:

$$I_\alpha(\mu) = \iint f(x,y)\,\delta(x\cos\alpha + y\sin\alpha - \mu)\,dxdy \qquad (3)$$

where δ is the Dirac delta function. The simplest surfacelet is the ridgelet transform

$$\Psi_{a,b,\alpha,\beta} = \left\langle I_{\alpha,\beta}(\mu), \psi_{a,b}(\mu) \right\rangle \qquad (4)$$

In general, our generic surfacelet transform is the 1D wavelet transform of the surface integrals.

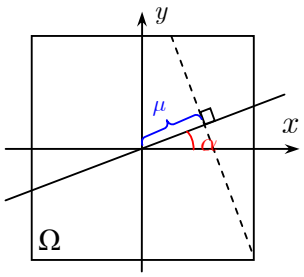

Fig. 1. Geometric interpretations of parameters in surfacelet transform.

3. Polymer Nanocomposite

We are interested in a nanocomposite system consisting of calcium-phosphorus (CaP) nanofibers in a polyhydroxybutyrate (PHB) matrix, (CaP/PHB). Figure 2 is the scanning electron microscopy image of CaP/PHB which was characterized for dispersion and distribution, thermal properties, and thermomechanical properties [6]. We use two methods to develop structure-property relationships. The multiscale microstructure model of CaP/PHB was represented using the surfacelet transform. We use the surfacelet model to recognize microstructural features, such as fibers, so that effective mechanical properties can be computed. By using the surfacelet transform, we can develop structure-property-geometry relationships.

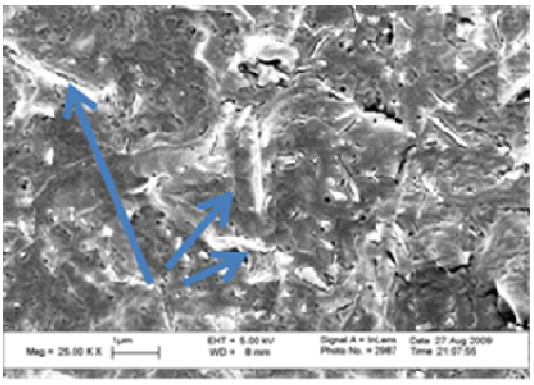

Fig 2. SEM images of nanofiber micro-structure (nano-fibers shown at tips of arrows).

The strain-stress relationship for a fiber in a polymer matrix microstructure can be derived readily from basic composite materials models for a single fiber in a polymer matrix [7]:

$$\varepsilon = \mathbf{S}\sigma = \begin{bmatrix} S_{11} & S_{12} & 0 \\ S_{12} & S_{22} & 0 \\ 0 & 0 & 2S_{66} \end{bmatrix} \begin{Bmatrix} \sigma_1 \\ \sigma_2 \\ \gamma_{12} \end{Bmatrix} \qquad (5)$$

where the S_{ij} are four independent constants in the elastic compliance tensor of a unidirectional laminate in its local frame (E_m = elastic modulus of matrix, E_{fi} = elastic modulus of fiber in direction i, G = shear moduli, ν = Poisson's ratio, V_r = volume fraction of fiber):

$$S_{11} = \left(E_m(1-V_r) + E_{f1}V_r\right)^{-1} \quad S_{22} = \frac{1-\sqrt{V_r}\left(1-E_m/E_{f2}\right)}{E_m}$$

$$S_{12} = \frac{\nu_m(1-V_r) + \nu_{f2}V_r}{E_m(1-V_r) + E_{f2}V_r} \quad S_{66} = \frac{1-\sqrt{V_r}\left(1-G_m/G_{f12}\right)}{G_m} \qquad (6)$$

The local compliance tensors can be transformed to global coordinates using the fourth-rank coordinate transformation law

$$S_{abcd} = Q_{ap}Q_{bq}Q_{cr}Q_{ds}S^l_{pqrs} \qquad (7)$$

where each Q_{ij} is a standard rotation matrix.

4. Simple Fiber-Reinforced Composite Example

The surfacelet representation and its hierarchical modeling capabilities are illustrated with a simple example of a fiber-reinforced composite material. Fig. 3 shows the sample microstructure, with vertical and horizontal fibers spaced 100 μm apart. We assume a typical carbon-epoxy composite material with property values of E_m = 2.94 GPa, E_{f1} = 234.6 GPa, E_{f2} = 13.8 GPa. The sample's elastic modulus

analytical model, surfacelet representation, 4X zoomed-out representation, and 4X zoomed-out elastic modulus model will be derived in this section.

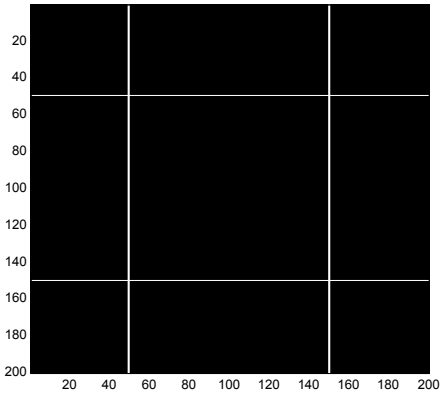

Fig. 3, Fiber-reinforced composite microstructure (dimensions in μm).

4.1 Surfacelet Representation

The Radon transform of the microstructure is shown in Fig. 4a, which illustrates the power of the transform for microstructures with linear elements. The four fibers from Fig. 3 are identified by the four bright spots in the Radon transform at (α,μ) = (0,50), (0,150), (90,50), and (90,150). The α values correspond to the angles of 0 and 90 degrees, while the μ values correspond to the positions of the fibers. Using the Radon transform, it is possible to convert line singularities (the fibers) into point singularities (the 4 bright points), effectively recognizing the presence of the fibers in the image. Applying the biorthogonal spline wavelet (bior1.3 in the Wavelet Toolbox) to the Radon transform yields the surfacelet representation shown in Fig. 4b.

To generate a larger-scale representation of this microstructure, wavelet decomposition operations are performed. The results after 4 such decomposition steps are shown in Fig. 4c. Note that the number of surfacelet coefficients has decreased by a factor of 16, a much lower resolution. Computing inverse wavelet and Radon transforms results in a reconstructed microstructure image, as seen in Fig. 4d. Note that the fibers are still visible in this image, indicating that the lower resolution did not disrupt the fiber representation.

Applying the mechanical property model in Eqns. 5-7, the effective elastic modulus is 5.85 GPa, which is close to a rule-of-mixtures approximation of 5.26 GPa, determined by interpreting the gray-scale values in Fig. 4d as material compositions.

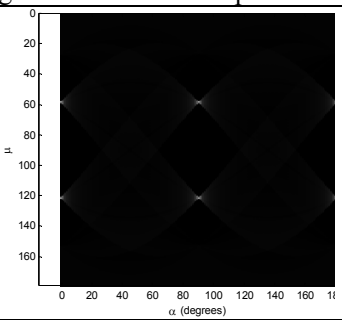

a) radon transform

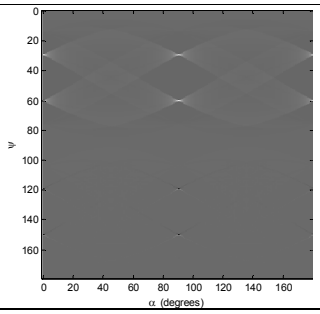

b) surfacelet representation

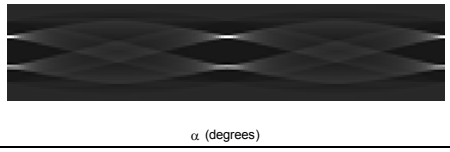

c) inverse wavelet transform after 4 levels of wavelet decomposition (compare with (a))

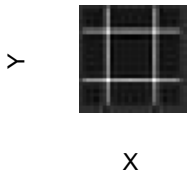

d) reconstructed image

Figure 4. Fiber-reinforced composite

5. Calcium-Phosphate Fiber Example

Nano-scale fibers represent one method for strengthening biopolymers for some applications. We will study CaP-PHB nanocomposite introduced in Section 3 with 5 weight-percent of CaP fibers. First, to demonstrate the ability to model microstructure, we will use a synthetic microstructure. Then, the surfacelet method will be applied to a micrograph of the actual material.

5.1 Three-CaP PHB fiber example

The properties of PHB are: E_m = 2 GPa, G_m = 1.2 GPa, ν = 0.4, density = 1.233 g/cm^3. The synthesized CaP nanofibers were on average 22 nm in diameter and 600 nm in length. Their mechanical properties were: E_{f1} = 110 GPa, $E_{f2} = G_{f12}$ = 10 GPa, ν = 0.3, and density = 2.22 g/cm^3.

Assuming that fibers are randomly distributed, a sample microstructure is shown in Figure 5a. Applying the model from Eqns. 5-7 and taking into account fiber orientations, the resultant elastic constant matrix is

$$\mathbf{E} = 1e9 \begin{bmatrix} 3.93 & 0.793 & 0 \\ 0.793 & 3.26 & 0 \\ 0 & 0 & 1.59 \end{bmatrix}$$

The rule-of-mixtures gives an effective elastic modulus of 3.45 GPa, which is known to overpredict moduli computed using more realistic models, while the inverse rule-of-mixtures provides a lower bound of 1.14 GPa, so our estimate is reasonable.

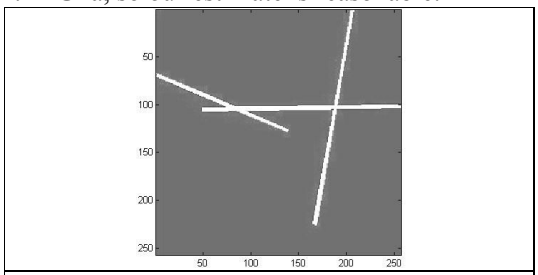

a) original image

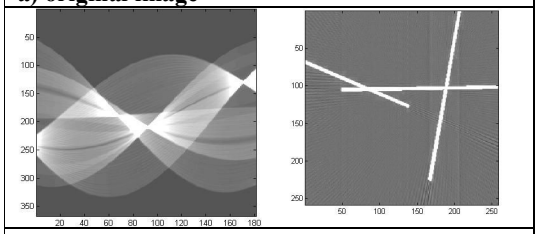

b) radon transform

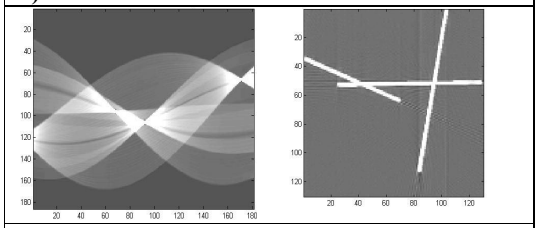

c) wavelet decomposition level 2

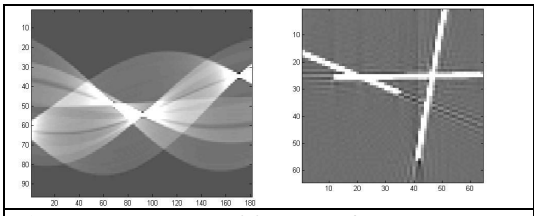

d) wavelet decomposition level 3

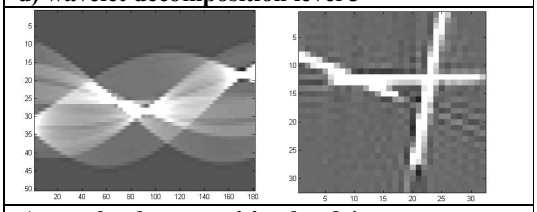

e) wavelet decomposition level 4

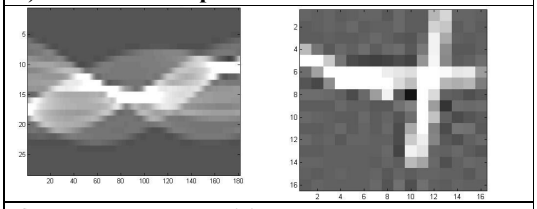

f) wavelet decomposition level 5

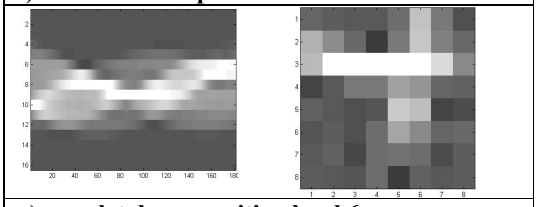

g) wavelet decomposition level 6

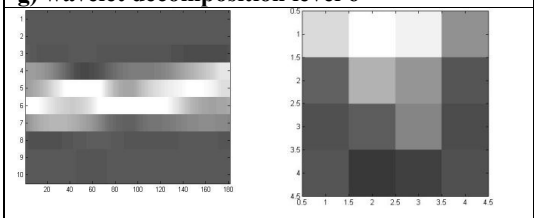

h) wavelet decomposition level 7

Figure 5, Three-CaP fiber image

Surfacelets were fit to Fig. 5a and wavelet decomposition was performed, enabling 7 levels of wavelet decomposition. The Radon transform is shown in Fig. 5b, along with the inverse surfacelet transform (inverse wavelet and inverse Radon transforms). Fibers can be recognized at the bright convergence points, which show that the fibers are at Radon transform angles of 92, 171, and 68 degrees. As shown in Fig. 5a, these angles are perpendicular to the actual fiber angles, which were at 2, 81, and 158 degrees, respectively. Again, the Radon

transform is effective in recognizing the presence of fibers in a microstructure image.

Figs. 5c-h show results of inverse wavelet and surfacelet transforms after 2-7 levels of wavelet decomposition. At 5-7 decomposition levels, too much resolution has been lost to adequately understand the Radon transform (inverse wavelet) or reconstruct fibers.

A total of 5 images were analyzed to better understand the effects of wavelet decomposition levels on microstructure images. The Radon transform (or inverse wavelet transform) results in a matrix of (α,μ) coefficients. The bright convergence points can be recognized by computing the standard deviation of coefficient values in each column and finding local maxima among them. Each column represents transform values at a single angle α for the range of positions μ. At the bright points, the coefficient values are very large, leading to large standard deviation values for those columns.

Table 1 shows the results for finding fibers in Radon transform images for the 5 randomly generated images, including the one in Fig. 5a (Image 3). The table entries indicate the average error between the actual fiber angle and the closest maximum in the standard deviation range. For example, entries of 0 indicate that all standard deviation maxima occurred exactly at the known fiber angles. Entries of 0.33 indicate that one out of three maxima was one degree away from the actual fiber angle. Results show that this analysis of Radon transform coefficient matrices can be used successfully to recognize fiber orientations at wavelet decomposition levels up to 4. At decomposition levels of 5 and above, the errors grow too large to reliably find fibers.

Table 1. Errors in finding fiber orientations.

Image	Radon	Decomposition Level of Wavelet Transform					
		2	3	4	5	6	7
1	0	0	0.33	0.67	3.00	12.33	8.33
2	0	0	0.33	0.67	2.00	3.33	7.67
3	0	0	0.33	1.00	3.67	10.33	14.00
4	0	0	0.33	0.67	3.00	12.33	8.33
5	0	0	0.67	1.00	2.33	8.00	21.67

5.2 Physical CaP-PHB example

The SEM micrograph of Fig. 2, of the 5 wt % CaP-PHB nanocomposite, is shown in Fig. 6 with 6 major fibers or fiber clusters circled. We hypothesized that the surfacelet transform would be able to model the fibers in a manner similar to that demonstrated in the synthetic images. The Radon and inverse surfacelet transforms are shown in Figure 7a-b. The inverse wavelet transform after 4 levels of wavelet decompression is shown in Fig. 7c, while the reconstructed image (inverse Radon transform of c) is shown in Fig. 7d.

Similarly to the synthetic microstructures presented earlier, it is possible to identify fibers as bright points in Fig. 7a and 7c. The angles found in Figs. 7a, c are 180, 46, 91, 123, and 138 degrees. Note again that these are 90 degrees from the actual fiber orientation due to the Radon transform definition. Each falls into the range of fiber angles estimated from Fig. 6. Table 2 shows the fiber angles found using the standard deviation maxima rule explained earlier. In the Radon transform and the inverse wavelet transforms from up to 4 levels of wavelet decomposition, it is possible to identify successfully the fiber angles. As a consequence, we can conclude that our hypothesis that the surfacelet transform would be able to model fibers in physical microstructures is validated.

6. Conclusion

A new hierarchical heterogeneous modeling method was described to model both the geometry and material information of parts. The model represents internal material distributions, microstructure boundaries, and part boundaries with a unified implicit form. Surfacelets as new basis functions were proposed to capture boundary information for both the part and the material microstructure (e.g., grain boundaries). A hierarchical modeling method of computing low resolution microstructures was tested that utilizes wavelet decomposition. The surfacelet model and method were demonstrated on several examples, a simple continuous-fiber-reinforced composite and several synthetic and natural nanofiber reinforced polymer material.

Modeling results indicated that material composition and microstructure, and their corresponding mechanical properties, could be integrated readily. A homogenization method was applied successfully to compute effective elastic properties from the

hierarchical model. The application of the wavelet decomposition method for computing low resolution models yielded good results. Fibers could be recognized in both the synthetic and natural microstructure images up to 4 levels of wavelet decomposition. At higher levels of decomposition, corresponding to lower resolutions, a rule-of-mixtures method could be used to compute effective mechanical properties

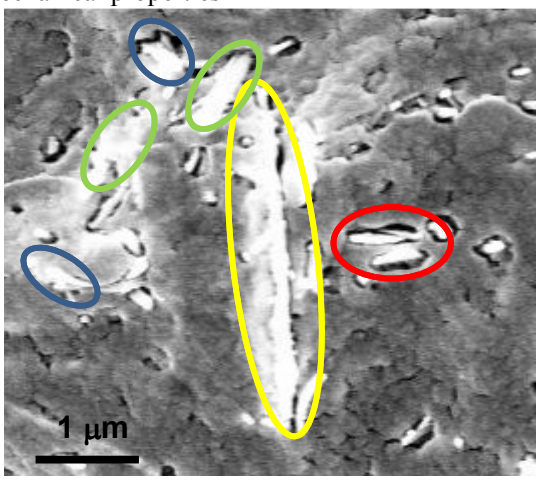

Figure 6. Micrograph of CaP-PHM composite with 5 wt % CaP fibers.

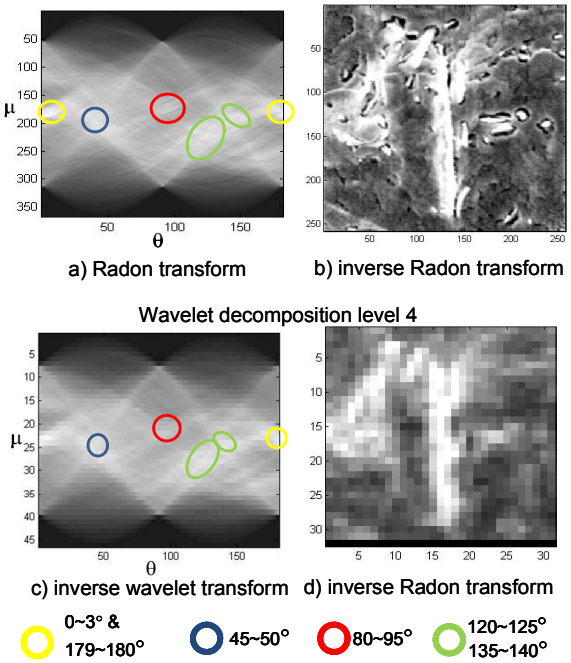

Figure 7. Surfacelet transform of CaP-PHB nanocomposite microstructure.

Table 2. Fiber angles in actual CaP-PHB microstructure

	179 ~3	45 ~50	85 ~95	120 ~125	135 ~140
Radon	180	46	91	123	138
Wavelet transform level 4	180	46	91	123	138

Acknowledgement

The authors gratefully acknowledge support from the National Science Foundation, grant CMMI-1030385. Any opinions, findings, and conclusions or recommendations expressed in this publication are those of the authors and do not necessarily reflect the views of the National Science Foundation.

References

[1] D. Rosen, N. Jeong, Y. Wang "A Hierarchical, Heterogeneous Material CAD Model with Application to Laser Sintering." *Solid Freeform Fabrication Symposium*, Austin, TX, Aug 9-11, 2010.

[2] Chui, C., Wavelet Analysis and its Applications, Vol. 1, Academic Press, Boston, 1992.

[3] Wang, Y., Rosen, D.W., "Multiscale Heterogeneous Modeling with Surfacelets," *Computer-Aided Design & Applications*, 7(5):759-776, 2010.

[4] Candès, E.J.: Ridgelets: theory and applications. Ph.D. dissertation, Stanford University, 1998.

[5] Kak, A.C., Slaney, M., *Principles of Computerized Tomographic Imaging*, SIAM, 2001.

[6] Kaur, J. (2010). *Properties of biologically relevant nanocomposites: effects of calcium phosphate nanoparticle attributes and biodegradable polymer morphology*. Atlanta, Ga.: Georgia Institute of Technology.

[7] Kalidindi, S.R. and J.R. Houskamp, "Application of the Spectral Methods of Microstructure Design to Continuous Fiber-Reinforced Composites," *Journal of Composite Materials*, vol. 41, pp. 909-930, 2007.